

# Factors affecting the adsorption of fatty acids, alcohols and aromatic compounds on to carbon black pigments (flow micro-calorimetry studies)

J.M. Peña<sup>a</sup>, N.S. Allen<sup>a,\*</sup>, M. Edge<sup>a</sup>, C.M. Liauw<sup>a</sup>, B. Valange<sup>b</sup>

<sup>a</sup>*Department of Chemistry and Materials, Manchester Metropolitan University, Chester Street, Manchester M1 6D, UK*

<sup>b</sup>*Cabot Corporation, Rue Prevostchamps 78, 4860 Pepinster, Belgium*

Received 5 October 2000; received in revised form 16 January 2001; accepted 22 January 2001

## Abstract

The surface activity of different types of carbon black with fatty acids, alcohols and aromatic compounds, is examined using flow micro-calorimetry (FMC), X-ray photoelectron spectroscopy (XPS) and Fourier transform infrared spectroscopy (FTIR). Significant differences in the overall adsorption activity of fatty acids and aromatic compounds are observed. The differences in behaviour between the various types of carbon black are evident and show that the specific surface area, as well as, their chemical nature are integral factors affecting the adsorption activity. Essentially, four factors were found to affect the adsorption activity of the fatty acids and alcohols: the presence of carboxylic and hydroxyl groups (which are found to form the strongest interactions with carbon black), the length and linearity of the hydrocarbon chain and the presence of unsaturation in the structure. Presence of aromatic ring type of functionality and size are also determinant factors in the adsorption of aromatic compounds. In order to characterise different carbon blacks, FTIR and XPS analysis have been used in an attempt to determine the nature of functional groups present on the surface of the carbon blacks. This provides valuable information regarding the adsorption mechanisms onto carbon black surfaces. Other techniques include thermogravimetric analysis (TGA), N<sub>2</sub> BET adsorption studies and Karl Fisher analysis. The latter tests were performed in order to determine differences in the volatile and water contents, respectively, of the carbon black samples. © 2001 Elsevier Science Ltd. All rights reserved.

**Keywords:** Carbon black; Adsorption; Flow microcalorimetry; Fatty acids

## 1. Introduction

In a previous series of papers [1–6] the influential factors in the adsorption/desorption processes of primary antioxidants, secondary antioxidants

HALS and acidic and basic model probes were studied in detail by the flow microcalorimetry technique (FMC).

These findings were also related to the efficiency of formulations containing such stabilisers in conjunction with carbon black, in a previous work concerning the thermal [7] and photostability of LDPE [8]. Thus, significant interactions between the CB and the stabilisers were reported. Both synergistic

\* Corresponding author. Tel.: +44-161-247-1482; fax: +44-161-247-6357.

E-mail address: n.allen@mmu.ac.uk (N.S. Allen).

and antagonistic effects were found, and seemingly the adsorption of the stabiliser was a major factor in determining the effectiveness of the HALS and primary and secondary antioxidants in the photostability of LDPE. In some cases, the presence of CB showed a retardant effect in the effectiveness of the stabilisers attributed to a process of adsorption followed by a progressive controlled release.

The effect of carbon black surface chemistry on interactions with stabilisers in thermoplastics based formulations relies on the chemical structure of the stabiliser and the surface chemistry of the CB. It has been also reported that chemical and physical interactions between carbon black surface groups and polar elastomer matrix chains were found to promote high reinforcement activity in many instances [9]. On the other hand, the adsorption of additives (stabilisers) onto fillers in thermoplastics is a recognised problem that is solved by using compounds, which sacrificially adsorb on to the filler surfaces thereby blocking the adsorption of the stabilisers [10].

Previous studies on other varieties of filler [11] indicated that the adsorption of stabilisers is not necessarily a negative feature and this can be used to provide what can be considered as a reservoir of stabilisers.

In order to attain a full understanding of the interactions between CB and additives in plastics formulations (such as plasticisers, stabilisers, etc), the study of the factors affecting the adsorption/desorption of fatty acids was essential as a model probe. This has been done by Flow micro-calorimetry (FMC) which has proved to be a useful technique for studying the interactions between carbon black and stabilisers in previous investigations [1–6,12].

However, the very complex physical structure of carbon black and the presence of numerous oxygen containing functional groups hamper attempts to obtain precise knowledge of the adsorption-desorption mechanism of stabilisers onto carbon black. The presence of impurities and adsorbed water can cause further complications in the surface analysis of carbon black. In general, furnace blacks contain 9 mg of oxygen per 100 m<sup>2</sup> of the surface [13]. Carbon blacks may contain as much as 1.2% combined sulphur, as well as ash at a few tenths of

a percent (sometimes as high as 1%). The ash consists of the salts and oxides of calcium, magnesium, sodium, and in some products potassium, and accounts for the basic pH 8–10 commonly found in furnace blacks [14]. Whilst hydrogen and sulphur are distributed on the surface and in the interior of the aggregates, oxygen is almost exclusively located on the surface in the form of carbon–oxygen functional groups. These groups have been identified as carboxyl, phenols, lactones, aldehydes, ketones, quinones, hydroquinones, anhydrides and ethereal structures [15].

Phenolic groups make up the majority of the surface oxygen content [13]. Hence, to find the CB parameters affecting its adsorptive capabilities, an in-depth characterisation of the pure CB grades used in this study was performed by FTIR, XPS, surface measurements (BET, Iodine adsorption), structure measurement (DBPA), and particle size (TEM).

The functional groups described above (carboxylic acid, phenolic, quinone and lactones), are believed to be attached to the edges of the graphitic layers. These groups can interact with elastomers and plastics as well as other additives such as plasticisers and stabilisers. By measuring the heat of adsorption, it has been shown that the interaction with various adsorbates is strong at very low coverage and decreases sharply once the level of coverage exceeds ca. 0.2 monolayers [16]. Inverse gas chromatography (IGC) and flow microcalorimetry (FMC) have revealed significant differences in adsorption energies and entropies, which are dependent on the shape of the hydrocarbon-adsorbate molecule and the structure and chemistry of the carbon black surface [17]. Polymer molecules are also adsorbed from solution onto the carbon black, and once adsorbed they are difficult to remove [4]. This is due both to strong bonding, at a small number of high energy sites, and to weak bonding at a large number of low energy sites, since desorption of a given polymer molecule requires simultaneous detachment of all the polymer-filler bonds [18].

Flow micro-calorimetry (FMC) has become an established method for characterising filler surfaces in terms of their surface chemistry and their interactions with surface treatments. The technique was initially used for this purpose by Fowkes [19] and later refined by Ashton and

Rothon [20]. FMC enables heats of adsorption and desorption to be measured and, with added concentration detectors, amounts adsorbed/desorbed can be obtained. The latter enables calculation of molar heats of adsorption–desorption.

## 2. Experimental

### 2.1. Materials

The fatty acids were selected in order of increasing aliphatic chain length and were: Acetic acid, valeric acid, hexanoic acid, octanoic acid, decanoic acid, stearic acid and oleic acid. Benzoic acid and phenol were the acidic aromatic compounds. Propan-1-ol, and octadecan-1-ol and ethyl acetate were the alcohols and ester analysed. Further details are given in Table 1.

The furnace carbon blacks CB-A, CB-B, CB-C and CB-D were all supplied by the Cabot-Corp. Their features are given in Table 2. It must be pointed out these carbon blacks were not treated with any form of binder. Therefore, the results reported reflect only the chemical nature and structure of the blacks. All other solvents/reagents (e.g. *n*-heptane) were of HPLC grade or 99% + purity where appropriate.

### 2.2. X-ray photoelectron spectroscopy (XPS)

The carbon black XPS spectra were obtained with a SSI-X probe (SS-100/206) spectrometer

from Fisons (Surface Science Laboratories, Mountain View, CA), equipped with an aluminium anode (10 kV, 17 mA) and a quartz monochromator. The direction of photoelectron collection made angles of 55 and 73° with the normal to the sample and the incident X-ray beam, respectively. The electron flood gun was set at 6 eV. The vacuum in the analysis chamber was  $2.5 \times 10^{-7}$  Pa. The binding energies of the peaks were determined by setting the C 1s component due to carbon only bound to carbon and hydrogen at a value of 284.2 eV. The peak areas were determined with a non-linear background subtraction. Intensity ratios were converted into atomic concentration ratios by using the SSI ESCA 8.3 D software package. The peaks were curve fitted using a non-linear least squares routine and assuming a Gaussian/Lorentzian (85/15) function.

### 2.3. FTIR, TGA and Karl Fisher procedures

Samples isolated from the FMC were air dried and then diluted to 0.09% w/w with dried KBr (3 h at 300°C), 0.2 g KBr discs were then pressed from these mixtures. KBr disks containing the pure carbon blacks were prepared in a similar manner. The samples were placed in a transmission cell fitted to a Nicolet 510 FTIR spectrophotometer (DTGS detector) with dry, CO<sub>2</sub> free air purge. Spectra were made up of 500 scans with a resolution of 2 cm<sup>-1</sup>. Thermogravimetric analysis (TGA) was performed in a nitrogen atmosphere using a Netzsch TG 209

Table 1  
Fatty acids, alcohols and aromatic probes investigated

Chemical structure	Molar mass	pK <sub>a</sub> <sup>b</sup>	μ <sup>a</sup> (debyes)	Chemical structure	Molar mass	pK <sub>a</sub> <sup>b</sup>	μ <sup>a</sup> (debyes)
Acetic acid	60.05	4.75 4.82	0.86	Benzoic ac.	122.03	4.19	(0.91) 1.45
Valeric acid	102.14	18°C	(0.86)	Phenol	94.11	9.89	(0.90) 1.68
Hexanoic acid	116.16	4.88	0.86	Propan-1-ol	60.1	≥ 17	(0.90) 1.6
Decanoic acid	172.27	4.96	(0.86)	Octadecan-1-ol	270.5	≥ 17.5	(0.90)
Stearic acid	284.49	4.9	1.75 (0.86)	Ethyl acetate	88.11	–	1.78 (0.052)
Oleic acid	282.47		(0.86)				

<sup>a</sup> Electric dipole moment in the gas phase [32].

<sup>b</sup> pK<sub>a</sub> values in aqueous solution [32] for bases is the value of conjugated acid.

in a nitrogen atmosphere, samples (6–12 mg) were heated from 25 to 900°C at 1°C min<sup>-1</sup>. The results gave the volatile content of the carbon black grades.

In order to determine the water content of the pure carbon blacks studied, Karl Fisher tests were performed with a Kyoto MKC210 titrator coupled to an ADP-351 evaporator at 200°C in 20 min.

#### 2.4. Flow micro-calorimetry

The FMC used was a Microscal 3Vi. Details of the downstream detector etc. are provided elsewhere

[21]. For the most of additives, the carrier fluid was heptane (Aldrich HPLC grade) stored over freshly activated (350°C, 3 h) 4A molecular sieves. Chloroform was used with additives which were insoluble in heptane, e.g. Tinuvin 622<sup>®</sup> because of its polar nature. The cell temperature was 27°C (±1°C). Probe concentrations of 0.03% w/v. The flow rate was 3.30 cm<sup>3</sup> h<sup>-1</sup> and carbon black sample size was 67.5 mg (±0.5 mg). Decahydronaphthalene was used as the non-adsorbing probe. Samples were left to equilibrate overnight at a carrier fluid flow rate of 0.033 cm<sup>3</sup> h<sup>-1</sup>. The flow rate was then increased to 3.3 cm<sup>3</sup> h<sup>-1</sup> and the system left to

Table 2  
Properties of carbon blacks studied

CB type	Surface area <sup>a</sup>		Particle size <sup>c</sup> (nm)	Iodine number (mg g <sup>-1</sup> )	DBPA pellets (cm <sup>3</sup> /100 g)	Volatile content <sup>c</sup> (%)	pH <sup>c</sup>	Water content <sup>b</sup> (wt.% CB)
	Stsa (m <sup>2</sup> g <sup>-1</sup> )	N <sub>2</sub> SA Multipoint (m <sup>2</sup> g <sup>-1</sup> )						
CB-A	86.8	107.1	22	119.6	96.6	1.5	8.5	1.01
CB-B	79.3	81.1	25	79.2	101.6	1	8.5	1.08
CB-C	85.1	113.2	25	78.2	72.5	3.5±1	2.5	2.56
CB-D	370.5	542.8	13	173.3	91.3	8.5-12	2.5	8.59

<sup>a</sup> Obtained by N<sub>2</sub> BET measurements.

<sup>b</sup> Obtained by Karl Fisher measurements.

<sup>c</sup> Obtained from (Cabot North American Technical report) [22].

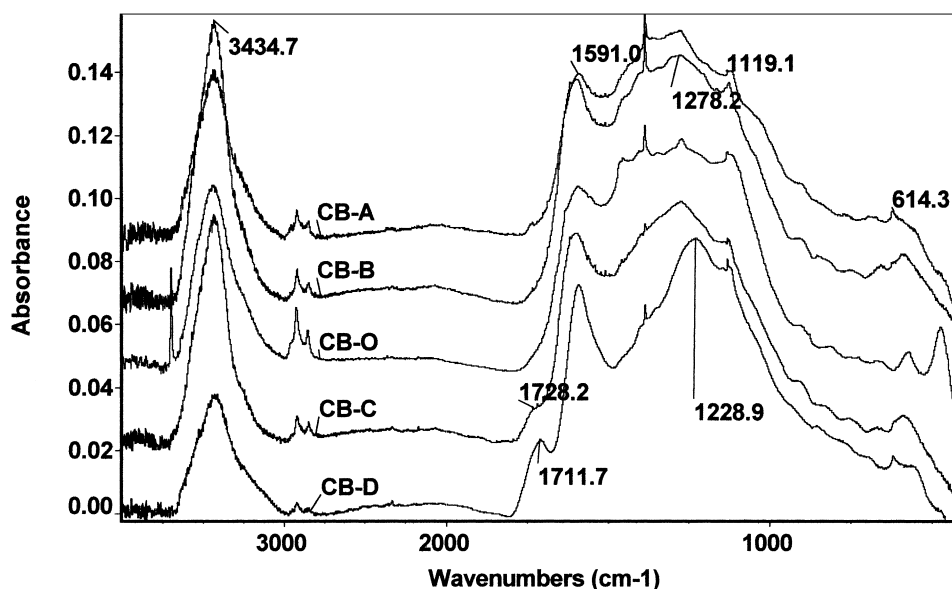


Fig. 1. FTIR spectra of CB-A, CB-B, CB-C and CB-D, pure carbon blacks.

settle for ca. 1 h. An overview of the FMC technique is provided by Ashton [20].

### 3. Results and discussion

#### 3.1. Characterisation of the carbon blacks

Chemical analysis of the carbon black surfaces was carried out using X-ray photoelectron spectroscopy (XPS), FTIR,  $N_2$  BET adsorption studies, Iodine adsorption and Karl Fisher measurements. Additional data were obtained from a Cabot North American Technical report [22]. The water content, volatile content and pH can be related to the hydrophilic character of the carbon black particle. For example, CB-D and CB-C have been oxidised with nitric acid and therefore have a higher surface concentration of oxygen containing functional groups than CB-B and CB-A. The FTIR and XPS analysis, which follows, effectively confirms the latter.

The differences between the  $N_2$  Stsa specific surface and the  $N_2$  (Multipoint) specific surface can be related to the porosity of the carbon blacks. Data shown in Table 2, together with literature data [23], indicates that CB-D is likely to have a porous surface. Micro-pores (< 2 nm), meso-pores and macro-pores are present in this sample and are likely to affect its adsorption behaviour.

##### 3.1.1. FTIR studies on pure carbon blacks

The FTIR results show that only CB-C and CB-D have a well-defined presence of functional groups on the surface, both (Fig. 1) have peaks that correspond to structures featuring carbonyl and carboxyl groups, however, CB-D shows a higher proportion of these groups.

In general, these spectra are similar to examples found in the literature [24,25]. The breadth of the carbonyl absorption band envelope (1735–1700  $cm^{-1}$ ) reflects a mixture of different groups attached to a polyaromatic structure (anhydrides, lactones (1735  $cm^{-1}$ ), aldehydes (1700  $cm^{-1}$ ). Due to the acidic nature of these two carbon blacks, some of these groups may be carboxylic acids (1700–1720  $cm^{-1}$ ). The XPS contribution at 531.5 eV corresponds to C=O (aldehydes, ketones and carboxylic

acids). These bands are still present in spectra of heptane washed samples recovered from the FMC cell, therefore these functional groups are likely to be chemically attached to the carbon black surface and not associated with physically adsorbed molecules. The deconvoluted XPS data is in agreement with and thus complements the FTIR data.

Other structures such as phenols, ketones, quinones, hydroquinones and anhydrides, may lay hidden within the broad absorption envelope of the C=C stretching vibrations of the polyaromatic structures of carbon black. However, such groups are detected by XPS at 534.5 eV which represent C–O linked to  $sp^2$  carbons (such as Ph–O or O=C–O). Moreover, as observed in the literature, the intensity of the band at 1600  $cm^{-1}$  increases as the volatile content increases, therefore, the infrared absorption described above includes some oxygen functionality.

CB-B and CB-A do not show a carboxylic acid group (1700–1720  $cm^{-1}$ ) (Fig. 12). The presence of phenolic (C–O stretch at 1224  $cm^{-1}$ ) and carbonylic compounds in both blacks can be located between 1150 and 1300  $cm^{-1}$  [25].

From FTIR data, extrapolated values from semi-quantitative analysis described by O'Reilly et al. [25] of COO– and C=O groups can be calculated and are close to the calculated values by titration for the studied blacks: CB-D (about 0.2–0.25 meq  $g^{-1}$  of COOH and 1.8 meq  $g^{-1}$  of C=O groups), CB-C ( $\leq$  0.1 meq  $g^{-1}$  of COOH and 0.5–0.75 meq  $g^{-1}$  of C=O groups) CB-B (about  $\leq$  0.7 meq  $g^{-1}$  of C=O groups) and CB-A (about 0.61 meq  $g^{-1}$  of C=O groups). No carboxylic acid groups were detectable on the latter two carbon blacks.

It is also evident that the presence of water in the carbon black and KBr gives rise to a broad OH stretching band, which obscures OH absorptions associated with phenolics and carboxylic acids. However, O'Reilly [25] has shown that no discernible phenolic OH bands were apparent at 3600  $cm^{-1}$ , even after subtraction of the OH absorption band from adsorbed  $H_2O$ .

##### 3.1.2. Analysis of carbon black surface chemistry by X-ray photoelectron spectroscopy (XPS)

From the global spectra, corresponding to the collection of electrons with binding energies

between 0 and 1100 eV, the surface elemental composition of each carbon black was estimated. In addition to carbon, the presence of oxygen and sulphur on each CB surface was detected. Nitrogen was also detected on CB-C and CB-D. Table 3 presents the percentage atomic fractions and the relative O/C, S/C and N/C ratios for direct quantitative comparisons between the CB samples.

From the O/C ratio, a direct indication of the extent of oxidation of the CB surfaces is obtained, and can be ranked as follows; CB-D > CB-C > CB-B > CB-A. There is a 10-fold difference between the lowest and highest surface oxygen concentration.

CB-A appears to be the “cleanest” black, as no nitrogen and only a very small quantity of sulphur can be detected. The level of oxidation of CB-A is very low and is reflected in the lowest surface oxygen concentration of all the samples examined. CB-B contains the highest sulphur level and has a surface oxygen concentration almost twice that of CB-A. The two highly oxidised samples, CB-D and CB-C, predictably, have the highest surface oxygen concentration. Some sulphur and nitrogen containing functional groups could also be detected on the surfaces of the latter two samples.

In order to identify and even quantify the different functional groups associated to O, N and S, high-resolution spectra of C(1s), O(1s), N(1s) and S(2p) photoelectrons were produced. These spectra have been deconvoluted so the contributions of the various functional groups, to the overall peak envelope, can be estimated [26].

Due to the polyaromatic nature of the carbon black, curve fitting of the C(1s) spectrum is difficult. The main C(1s) component at 284.2 eV, corresponding to non-functionalised carbon (i.e. C–C, C–H), shows unusual asymmetry which was impossible to model with the processing program used. This asymmetry also affected the compo-

nents at higher binding energies (carbons linked to heteroatoms). If curve fitting is performed regardless of this asymmetry, over-estimation of contributions, arising mainly from oxidised carbons (i.e. O–C, O=C, O–C=O) occurs. Rather than trying to correct this analytical error by attempting to model this asymmetry (which would be a computationally intense process), a deeper interpretation and discussion based on the oxygen (O(1s)) peak was preferred.

Fig. 2 displays high-resolution spectra of oxygen (O1s) for all the carbon black samples. Peak areas are directly proportional to the atom fraction. In addition to the simple increase of extent of oxidation from CB-A to CB-D, deduced earlier from O/C ratios, the O(1s) spectra indicate qualitative variations in the nature of the oxygen content. For CB-C and CB-D, the O(1s) peak exhibits an important shoulder at lower binding energies resulting from the presence of functional groups produced under strongly oxidising conditions. In order to proceed further in this qualitative interpretation, deconvolution curve fitting of these high-resolution spectra, using the previously described parameters, has been performed. Fig. 3 summarises the curve fitted and deconvoluted spectra for all the samples considered.

CB-A gave a simple curve with two components near 533 eV and 536 eV respectively. The former corresponds to C–O functional groups (mainly ethers/hydroxyls linked to sp<sup>3</sup> carbon) and the latter results from adsorbed species (H<sub>2</sub>O and O<sub>2</sub>). The O(1s) peak of CB-B is deconvoluted into the same contributions at 533 and 536 eV. However, a third component, associated with satellite ( $\pi$ – $\pi^*$ ) shake-up, appears at 537.6 eV, and thus explains the more pronounced shoulder appearing at higher binding energies. Interpretations of the CB-C and CB-D curves were more complex but similar features to CB-A and CB-B remained apparent. However, with CB-C and CB-D, two additional components at 531.5 and 534.5 eV were present. Oxygen at 534.5 eV represents C–O linked to sp<sup>2</sup> carbons (such as Ph–O or O=C–O). The contribution at 531.5 eV corresponds to oxygen with a high density of bonding electrons; they can be associated to C=O (aldehydes, ketones, carboxylic acids) or S–O (sulfoxes, sulphates).

Table 3  
Surface elemental compositions of the different carbon blacks

CB sample	% C	% O	% S	% N	O/C	S/C	N/C
CB-A	99.44	0.55	0.02	0	0.0055	0.0002	0
CB-B	98.48	0.96	0.54	0	0.0097	0.0055	0
CB-C	95.54	3.73	0.34	0.39	0.0390	0.0036	0.0041
CB-D	93.8	5.77	0.23	0.18	0.0615	0.0025	0.0019

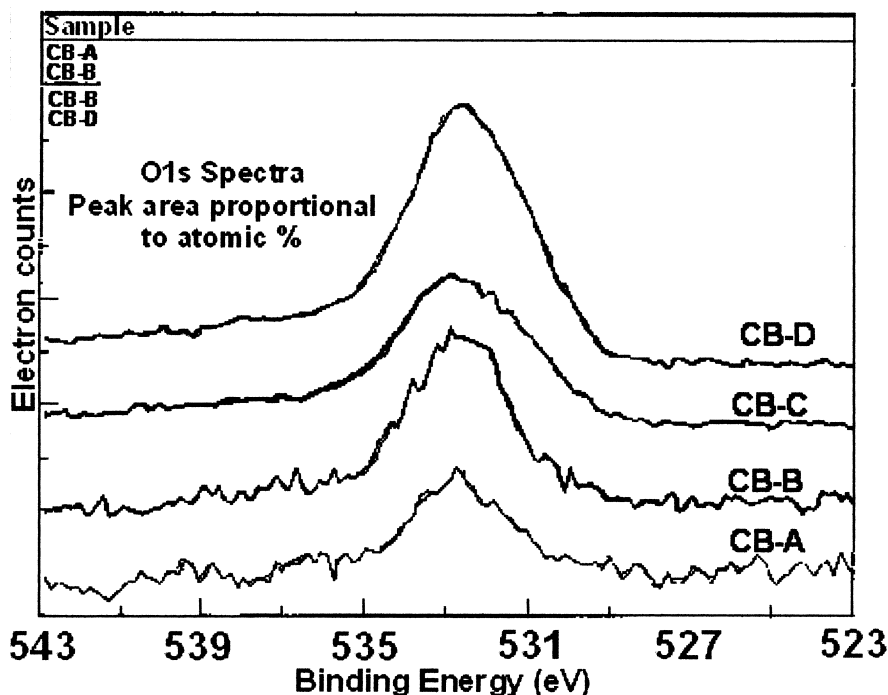


Fig. 2. O1s spectra of CB-A, CB-B, CB-C and CB-D. Peak area proportional to % O.

The different S2p spectra are grouped in Fig. 4. Again, from their high-resolution spectra, we observed significant differences in the sulphur contents of the carbon blacks. As with the O(1s) data, curve fitting and deconvolution was performed in order to gain further insight into the chemical nature of the sulphur containing functional groups. The CB-A curve indicates a very small component at 163.8 eV, corresponding to  $\underline{\text{S}}\text{-C}$ . This component is also present on the other three samples and the relative levels of  $\underline{\text{S}}\text{-C}$  based species can be ranked as follows: CB-B > CB-C > CB-D. On these latter carbon blacks, two other sulphur-containing moieties were detected. The first appears at 166.4 eV and corresponds to sulphones and the second appears at 168.8 eV and is due to sulphates. The level of  $\text{SO}_4$  can be ranked as follows: CB-D > CB-C > CB-B, this trend is exactly opposite to that for  $\underline{\text{S}}\text{-C}$ .

Finally, an estimate was made of the relative amount of each chemical species identified respectively in the fitting studies, by combining them with the quantitative elemental composition described earlier in Table 1. In other words, the global O

and S content can be split into their different components. The detailed results are reported in Table 4. It is important to emphasise that the values obtained mathematically from deconvoluted data are dependent on user-defined parameters which are selected to provide a realistic fit to the experimental data.

Given the considerations reported by Papirer [26] concerning the relative particle size ( $d$ ) and the depth of escape of the photoelectrons ( $x$ ) by which  $x \cong d = 15\text{--}20$  nm; we can assume that the amounts of oxygen, sulphur and nitrogen estimated would coincide with the estimations of compositions made by chemical analysis. According to our FTIR results, oxygen-containing groups were detected on the surface of the carbon blacks, and it can be concluded that these functional groups are located on the CB surface, as reported in the literature [13]. The sulphur levels obtained from XPS are different to those reported in the bibliography [13], where the presence of sulphur is distributed within the bulk of the carbon black. However, if the sulphur is equally spread in all the blacks, the results in different samples of CB will be valid in order to compare the relative sulphur content.

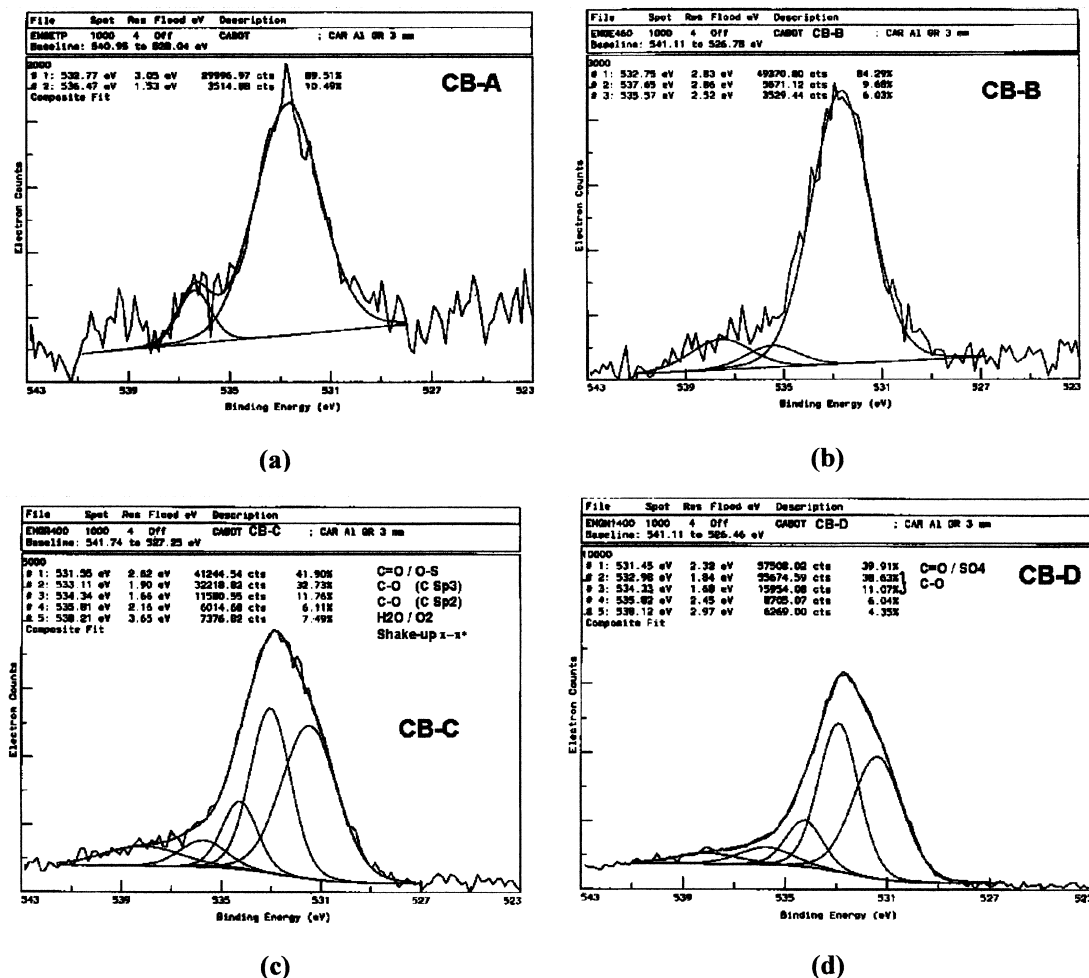


Fig. 3. High resolution fitted O1s spectra: (a) CB-A, (b) CB-B, (c) CB-C, (d) CB-D.

### 3.2. Adsorption of fatty acids onto the carbon black samples

Different fatty acids, carboxylic acids, alcohols and carbon blacks were chosen according to their chemical nature and surface features. CB-A and CB-B, are both used in plastic applications, while CB-C and CB-D are nitric acid treated CBs for specialised applications. First of all, their interaction with acidic model compounds such as phenol, acetic acid and so on, were examined in order to compare the difference in activity of the four blacks with these compounds as a function of their acidic character and structure. Following this several

fatty acids are compared to study the effect of the chain length and structure on their interactions with carbon black. For ease of comparison, the results are presented as a histogram showing adsorption and desorption data for each probe, with the sign of the exothermic adsorption energy change being reversed (adsorption energy).

#### 3.2.1. Adsorption energies of carboxylic acids alcohols and ethyl acetate

Adsorption and desorption energies resulting from the interactions of the different acidic probes with the carbon blacks were determined by the FMC procedure. Figs. 5 and 6 show that, in general



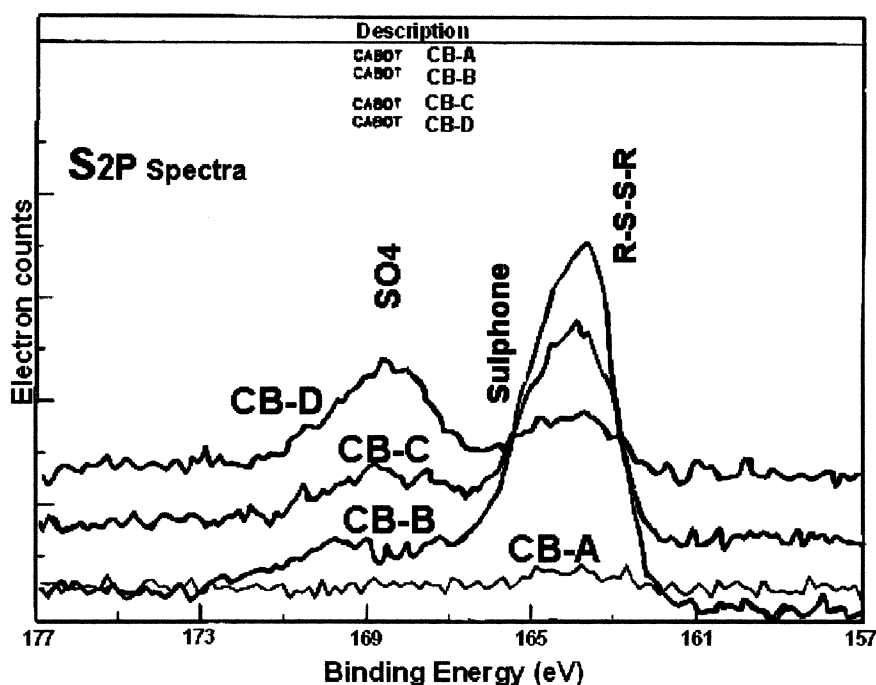


Fig. 4. S2p spectra of CB-A, CB-B, CB-C and CB-D. Peak area proportional to % S.

Table 4  
Detailed functional composition (ratio O/C, S/C) of the different carbon blacks

Sample	O=C O-S Carboxylic aldehyde, ketone,	O-C Hydroxyl, ethers	O-C Phenol anhydride	H <sub>2</sub> O O <sub>2</sub>	S-C	SO <sub>2</sub> Sulphones	SO <sub>4</sub> Sulphates	C-N	NO <sub>2</sub>
Binding energy	531.5 eV	533.1 eV	534.5 eV	535.8 eV	163.8 eV	166.4 eV	168.8 eV	400 eV	405 eV
CB-A	0	0.0049	0	0.0006	0.0002	0	0	0	0
CB-B	0	0.0082	0	0.0006	0.0043	0.0006	0.0003	0	0
CB-C	0.0163	0.0127	0.0046	0.0024	0.0023	0.0005	0.0006	0.0027	0.0014
CB-D	0.0245	0.0238	0.0068	0.0037	0.0008	0	0.0016	0.0019	0

the greater acidic character of a model compound the greater adsorption activity on a given carbon black, with the exception of stearic acid, which shows a lower adsorption activity than phenol.

The acidic character of the additives used can be ranked as follows:

Benzoic acid ( $pK_a \approx 4.2$ ) > stearic acid ( $pK_a \approx 5$ )  
> phenol ( $pK_a \approx 10$ ) > propan-1-ol ( $pK_a \approx 17$ –16)  
≥ octadecanol ( $pK_a \approx 17$ –16).

Ethyl acetate obviously has no  $pK_a$  value, but will be able to interact by dipolar interaction. Despite the fact that stearic acid has a higher acidity, phenol shows the highest adsorption energy, followed by benzoic acid. This higher activity is probably due to the flat and planar aromatic structures of the latter two probes (Figs. 9 and 10), as opposed to the C<sub>17</sub> alkyl chain of stearic acid. The latter portion of the stearic acid molecule accounts for the major proportion of its molecular volume,

and will have strong affinity for the heptane carrier fluid, therefore strong solvation of the alkyl chain is likely. Detachment of the solvating molecules (endothermic) during adsorption will decrease the heat of adsorption. The more compact benzoic acid (Fig. 9) and phenol molecules may also easily fit into the pores of CB-C and CB-D, thus allowing a greater surface area for adsorption. This explanation can be also applied to propanol and octadecanol (Fig. 11); because with CB-C and CB-D, the heat of adsorption of the latter probe was noticeably less than the former one. This reasoning

breaks down with CB-A and to a lesser extent with CB-B, due to the previously described surface topological differences.

Differences in the heats of adsorption of octadecanol and stearic acid afford some insight into the nature of the interaction and hence the type of surface functional group with which it interacts. On CB-C, the adsorption energies of these two probes are very similar, whilst with CB-D, octadecanol is the more strongly adsorbing probe. This could be explained on the basis of the amphoteric character of the alcohols, which may result in the octadecanol

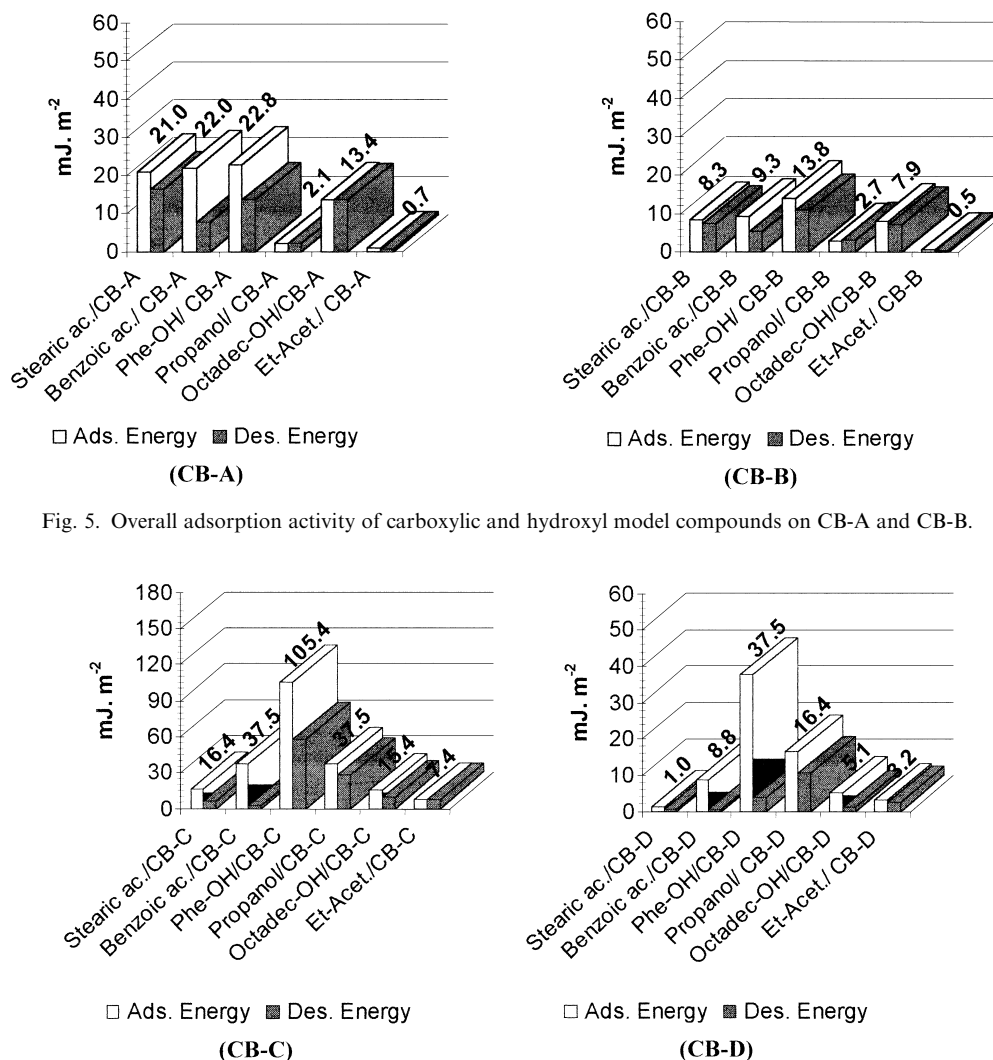


Fig. 6. Overall adsorption activity of carboxylic and hydroxyl model compounds on CB-C and CB-D.

and propanol acting as bases for the relatively strong acids located on the carbon black surface [27]. Such an effect will cause the heat of adsorption to exceed that of stearic acid, which can only interact with the surface acid groups by hydrogen bonding. This explanation can also be applied to the differences observed between phenol and benzoic acid when adsorbed onto CB-D and CB-C.

With CB-A and CB-B the adsorption energies of stearic acid, phenol and benzoic acid are quite similar, this may be due to similarity in the

adsorption mechanism for each of these probes. With CB-B these adsorptions were shown to be reversible which implies that hydrogen bonding and dispersive interactions are mainly involved, rather than acid–base interactions. However, with CB-A phenol and benzoic acid showed greater retention that may reflect stronger dispersive interactions, resulting from the previously described flat adsorption of these probes (Fig. 12). In contrast, the same probes showed far stronger retention on CB-C and CB-D, therefore indicating a strong contribution from acid–base interactions.

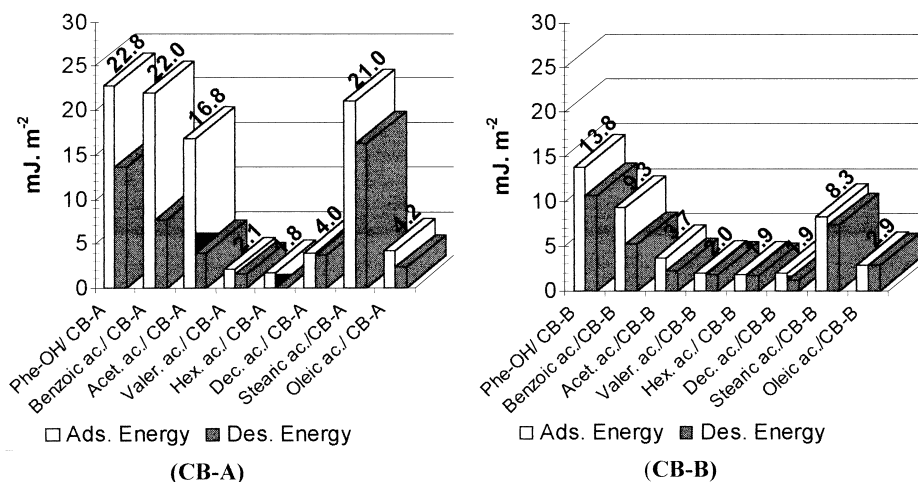


Fig. 7. Overall adsorption activity of fatty acids on CB-A and CB-B.

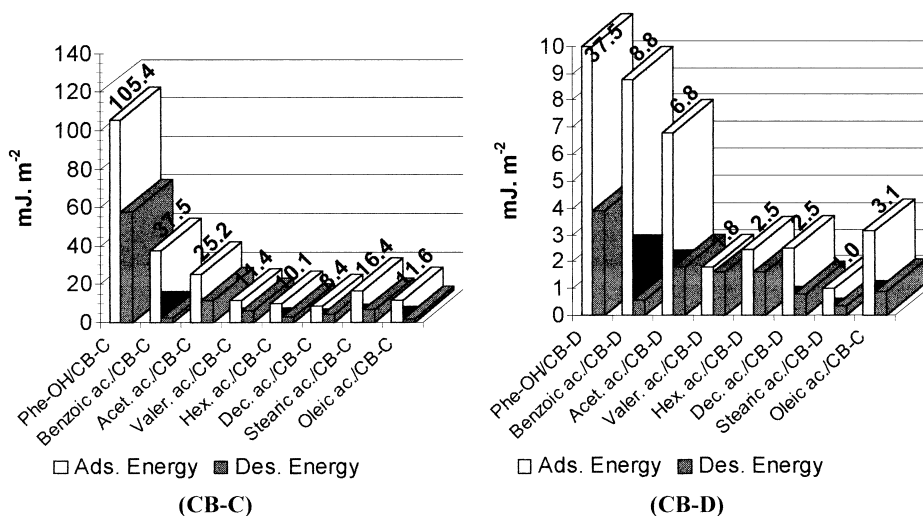


Fig. 8. Overall adsorption activity of fatty acids on CB-C and CB-D.

Resonance stabilisation of the phenoxide ion causes phenol to be more acidic than aliphatic alcohols; this feature enhances the adsorption activity of phenol relative to octadecanol and propanol [27]. The similar adsorption energy trends observed with phenol and propanol, and the relative differences between propanol and stearic acid, across the four carbon blacks examined, can be explained by the differing adsorption mechanisms

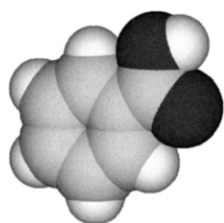


Fig. 9. 3D minimal energy structure of benzoic acid.

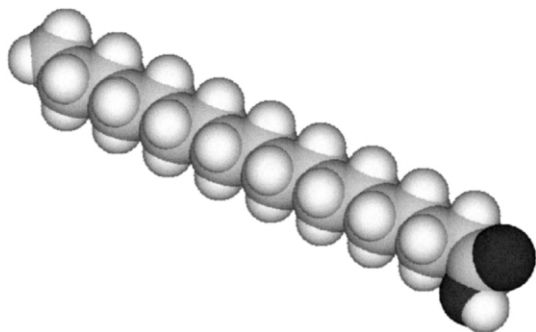


Fig. 10. 3D minimal energy structure of stearic acid.

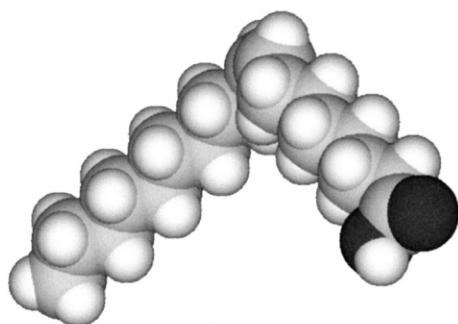
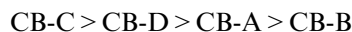


Fig. 11. 3D minimal energy structures of oleic acid.

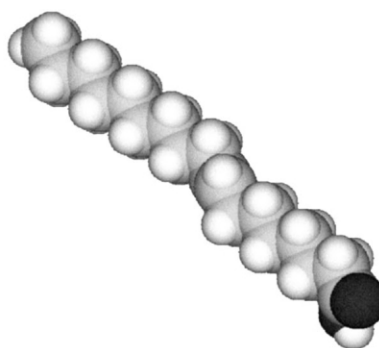
of these probes. Although phenol is likely to have a stronger acid-base component to its energy of interaction, relative to propanol, both these alcohols are able to interact with the carbon black via hydrogen bonding. Being flat and planar with delocalised  $\pi$ -electrons, the aromatic ring of phenol can participate in dispersive interactions when it is adsorbed flat on to the graphene layers of carbon black. Fig. 12 is a model of the adsorption of phenol on a graphene layer containing a phenolic group. The figure represents the modelled state of lower energy in the interaction phenol–phenolic–CB resulting in a flat wise adsorption. The effects on the phenol adsorption have been discussed in the literature [28] and will further increase the energy of adsorption.

Ethyl acetate interacts weakly with carbon black via the ester grouping, which may participate in hydrogen bonding with labile hydrogen atoms of acidic sites on the carbon black surface. Such sites include carboxyl groups (evident on CB-C and CB-D, Fig. 1) and phenolic groups (Table 4). Ethyl acetate shows the weakest adsorption activity with CB-A and CB-B, due to the very low surface concentration of acidic functional groups on these samples.

With all four carbon blacks, identical adsorption energy trends are observed with phenol, propanol and ethyl acetate. The ranking is as follows:



(with the exception of CB-B which shows a slightly higher adsorption energy with propanol than CB-A)



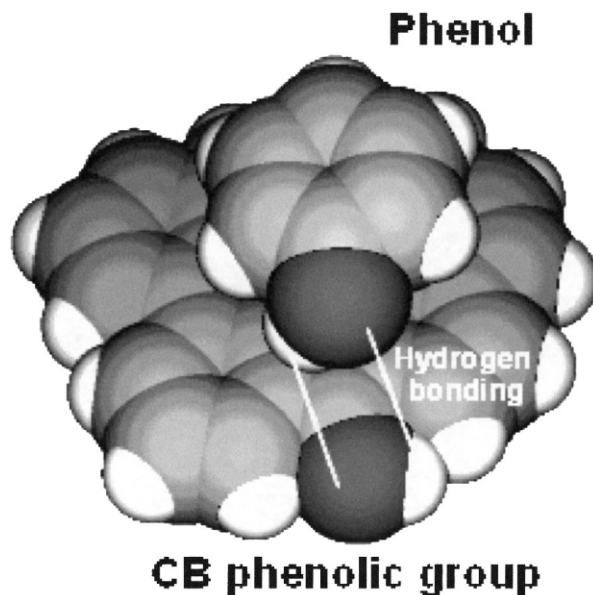


Fig. 12. 3D interaction between phenol and a carbon black phenolic group. Minimal energy structures of both molecules.

The actual values of adsorption energy can be ranked as follows:

with phenol:  $(105.4 \text{ mJ m}^{-2}) > (37.5 \text{ mJ m}^{-2}) > (22.8 \text{ mJ m}^{-2}) > (13.8 \text{ mJ m}^{-2})$ ,  
 with propanol:  $(37.5 \text{ mJ m}^{-2}) > (16.4 \text{ mJ m}^{-2}) > (2.1 \text{ mJ m}^{-2}) > (2.7 \text{ mJ m}^{-2})$ ,  
 with ethyl acetate:  $(7.4 \text{ mJ m}^{-2}) > (3.2 \text{ mJ m}^{-2}) > (0.7 \text{ mJ m}^{-2}) \geq (0.5 \text{ mJ m}^{-2})$ .

Variation of the surface acidity (Bronsted) of the carbon blacks, cannot in itself, explain the ranking observed, as the Bronsted acidity can be ranked as follows:

$\text{CB-D} \geq \text{CB-C} > \text{CB-B} \geq \text{CB-A}$ .

It is important to appreciate that basic groups can also be present on the surface. The carbon black surface should hence be considered amphoteric in nature. Different ratios of concentration of basic/acidic groups on the carbon black surface could explain the data presented in Figs. 5 and 6. Due to the acidic character of the compounds, the higher activity of a given carbon black could be interpreted by a greater presence of selective basic

active adsorption sites per unit surface area on that carbon black.

As the adsorption energy of stearic acid on to the four carbon blacks can be ranked as follows,

$\text{CB-A} > \text{CB-C} > \text{CB-B} > \text{CB-D}$ ,  $(21.0 \text{ mJ m}^{-2}) > (16.4 \text{ mJ m}^{-2}) > (8.3 \text{ mJ m}^{-2}) > (1.0 \text{ mJ m}^{-2})$ .

It may be suggested that CB-A has a higher surface concentration of basic sites than CB-C etc.

FMC studies on a series of amines [5] and the surface chemical analysis evidenced that CB-C has the most effective acidic surface. However, CB-C also appears to have a significant concentration of basic sites on its surface as it shows the second highest adsorption energy with stearic acid.

The activity of CB-D appears to be weakened by the “hydrogel effect” and mutual interactions between functional groups. Whilst the high porosity of CB-D does not significantly affect the general adsorption energy trends with the acidic probes, the retention of phenol on CB-D is stronger than with any of the other samples. Such an anomaly may be due to phenol becoming trapped within the pore structure [28]. This effect is likely to be even

more pronounced if the phenol is partially dissociated in some of the strongly adsorbed water on the surface of CB-D. This will in turn result in interaction between the phenoxide ion and hydrogen atoms, which form the edges of the graphene layers that make up the walls of the pores.

CB-A and CB-C show very similar behaviour with stearic acid, both in terms of the adsorption energy and the level of adsorption (Figs. 4 and 5). It may, therefore, be argued that these samples have a significant surface concentration of basic sites. The exact form of these basic sites is hard to predict. However, for CB-A they may be associated with the  $\pi$ -electron systems of the polyaromatic graphene layers, which will act as Lewis bases [13,15]. By virtue of the relatively high purity of CB-A, the graphene layers are likely to be more perfect (i.e. flatter) than with the other samples.

This may result in structural (perhaps crystalline) ordering of the adsorbate molecules; the resulting intermolecular interactions will simultaneously increase both the energy of and level of adsorption. It is also interesting to note that on CB-A, the heat of adsorption of octadecanol is substantially higher than propanol. This observation may be explained by heat of crystallisation of the alkyl tails (or increased dispersive interaction caused by horizontal adsorption) and may thus be further evidence in support of adsorption on the graphene layers. With CB-C hydrogen-bonding interaction with stearic acid cannot be ruled out, though there may be some contribution from  $\pi$ -electron Lewis bases. Adventitious metal oxides originating from the feed-stocks themselves and process water used in production of the carbon blacks could also form Bronsted basic sites.

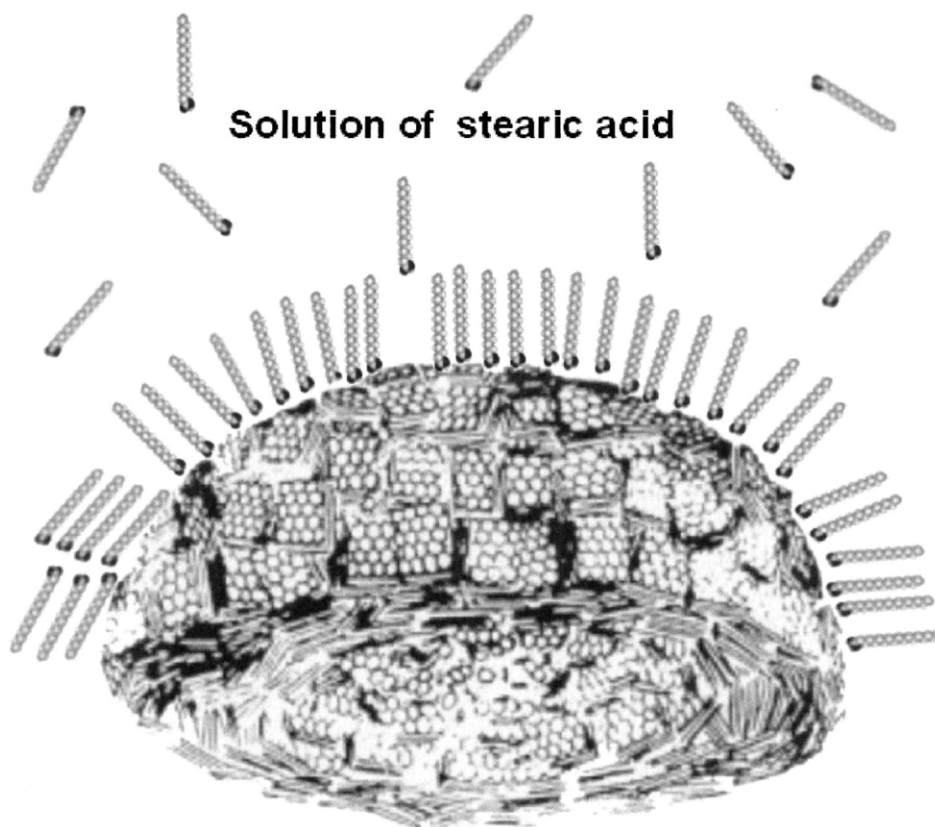


Fig. 13. Scheme of the possible adsorption of linear long chain fatty acids on the carbon black surface.

### 3.2.2. Overall adsorption activity of fatty acids

Adsorption and desorption energies resulting from the interactions of the different fatty acids with the carbon blacks by FMC are presented in Figs. 7 and 8. The adsorption energy for phenol and benzoic acid are also included to study the presence of the aromatic structure in the adsorption activity of carboxylic group.

A similar trend is observed for the CB-A, CB-B, and CB-C with all the acids. Aromatic acidic compounds show a higher adsorption activity than aliphatic compounds for all the CB's.

From our previous experiments with AOX1, HALS and acidic and basic model compounds [1–5], the type of interactions expected can be mainly H bonding [29] between the fatty acid carboxylic moieties (oxygen and H) with the H and the oxygen moiety respectively from carboxylic and phenolic groups attached on the CB surface. The aliphatic structures can also interact via Van der Waals forces with the carbon black surface.

As was described above, phenol shows the highest adsorption energy, followed by benzoic acid. This is despite the fact that the fatty acid exhibits higher acidity than phenol, because of the flat and planar aromatic structures of the latter two probes (Figs. 9–11), as opposed to the alkyl chain of the fatty acids. In the case of the decanoic, stearic and oleic acids, the latter portion of the fatty acid molecule accounts for the major proportion of its molecular volume, and will have strong affinity for the *n*-heptane carrier fluid, therefore strong solvation of the alkyl chain is likely. Detachment of the solvating molecules (endothermic) during adsorption will decrease the heat of adsorption. The more compact benzoic acid and phenol molecules may also easily fit into the pores of CB-C and CB-D, thus allowing a greater surface area for adsorption.

Fig. 12 represents a model of the adsorption of phenol on carbon black, by interacting with a phenolic group on the edge of a graphene layer. Phenol is adsorbed flat wise. The hydroxyls groups

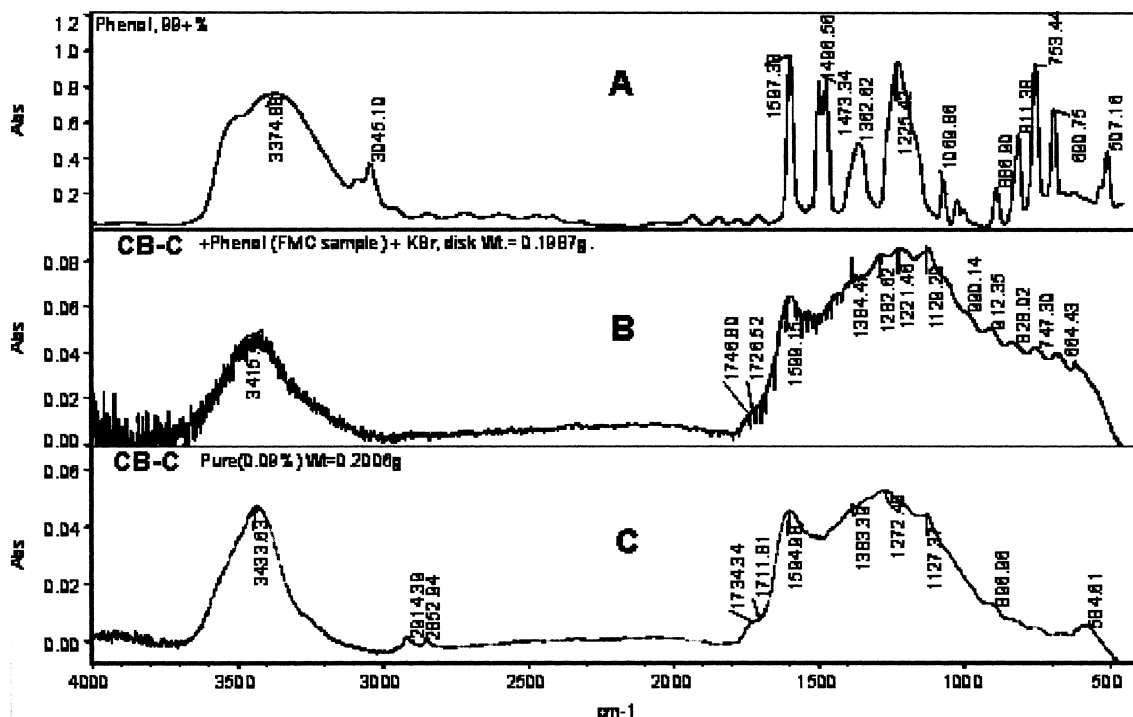


Fig. 14. Comparative FTIR spectra of: (A) pure phenol, (B) CB-C modified with phenol by FMC adsorption, (C) pure CB-C carbon black.

are aligned via hydrogen bonding, and the aromatic ring is parallel to the graphene layer, probably interacting via dispersive interactions.

These results agree with the literature [12], where adsorption activity was found to be influenced by molecular shape. Flat-shaped molecules as such showed a higher adsorption activity than those that are square shaped and this was confirmed in previous studies with stabilisers [3–6].

For smaller molecules such as acetic acid, for which the chain length cannot be accounted for in the differences observed with phenol and benzoic acid, their lower adsorption activity can be interpreted by the absence of the aromatic structure.

Increasing chain length from acetic acid to decanoic acid reduces the adsorption activity in the more acidic CBs (CB-B, CB-C and CB-D), except valeric acid for CB-D. For CB-A this is also true from acetic acid to hexanoic acid, with decanoic acid slightly more active. This could be explained by an increasing solvation of the aliphatic chain and hence a higher volume of the fatty acid molecule

being less accessible to the CB porosity, when the acidity does not change substantially (Table 1).

However a further increase of the chain length reverses this effect. Thus, stearic acid (Fig. 10) is more active than its relatives (from hexanoic to decanoic acid) with CB-A, CB-B and CB-C. With CB-A and CB-B, stearic is even more active than acetic acid, while with CB-B the adsorption activity of the former is close to that of the acetic acid. A similar observation was described above with octadecanol. A probable interaction between the aliphatic chains of the adsorbed molecules of stearic acid and the octadecanol can result in an ordered distribution by crystallisation of the alkyl tails perpendicularly or flat wise to the carbon black surface (Fig. 13). In such form the molecules of stearic acid would be adsorbed forming a layer similar to the structure found in micelles. Such an interaction could be via van der Waals forces between the aliphatic chains in addition to the hydrogen bonding of the acid group with the carbon black surface functionalities. Hence the balanced adsorption

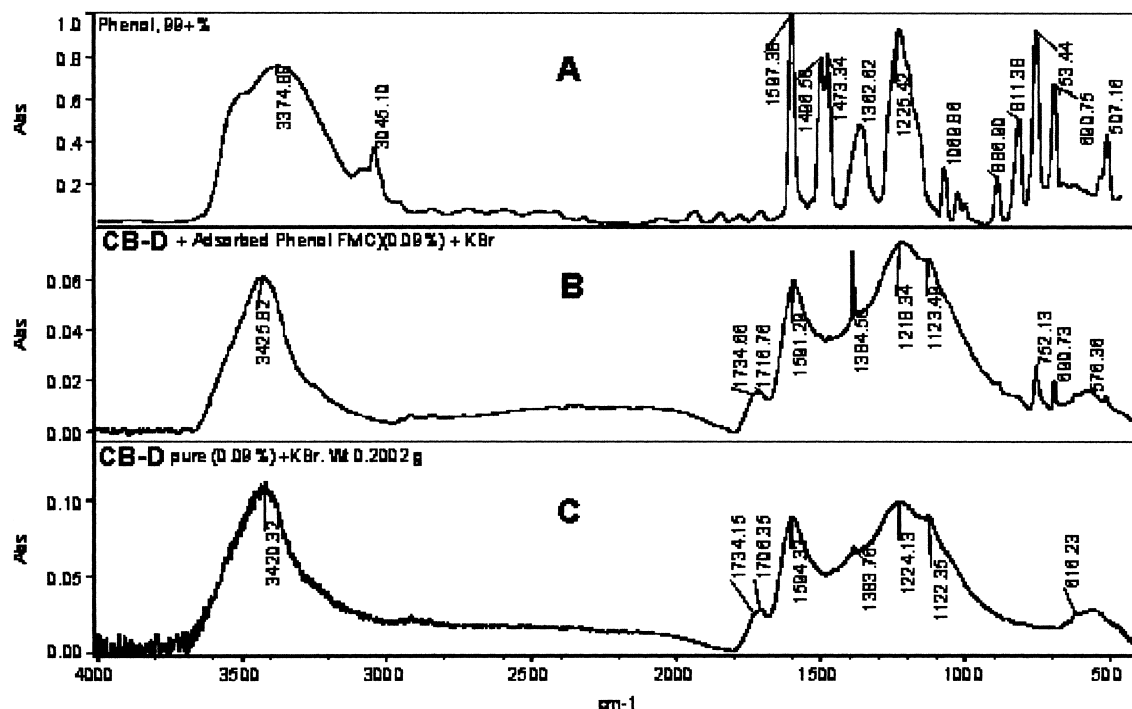


Fig. 15. Comparative FTIR spectra of: (A) pure phenol, (B) CB-D modified with phenol by FMC adsorption, (C) pure CB-D carbon black.



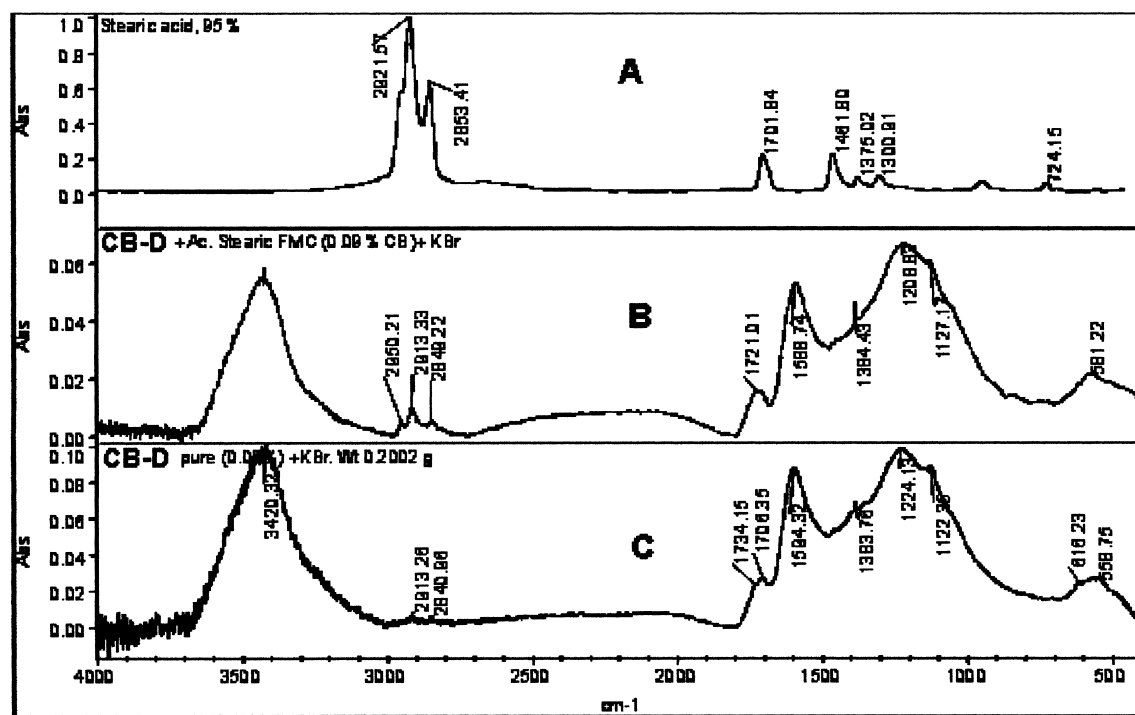


Fig. 16. Comparative FTIR spectra of: (A) pure stearic acid, (B) CB-D modified with stearic acid by FMC adsorption, (C) pure CB-D carbon black.

energy for stearic acid would be greater than for acetic acid, by heat of crystallisation of the alkyl tails (or increased dispersive interaction caused by horizontal adsorption).

The linear structure and length of the aliphatic chain of the fatty acid molecule are the conditions to obtain a more ordered adsorption and therefore a higher energy of adsorption. The lower adsorption energy for oleic acid (Fig. 11) compared with stearic acid (Fig. 10), with equal chain length, seems to be related to the loss of linearity because of the unsaturation in the middle of the former hydrocarbon chain. Thus, oleic acid cannot be adsorbed forming ordered layers, with the acidic group pointing to the CB surface. In that situation oleic acid shows close adsorption energies to their relatives, namely decanoic acid and hexanoic acid, because of the solvation effect and a less ordered adsorption than stearic acid.

In order to obtain a higher adsorption for a fatty acid or alcohol a linear aliphatic chain is therefore

required of a length equal or superior to  $C_{17}$ . It is also evident from Figs. 7 and 8 that there are important differences in relation to the adsorption/desorption activity between the four carbon blacks with the same additives. The CB surface structure, mainly the porosity, can play an important role in the ordered adsorption of fatty acids such as stearic acid. For instance, the inhomogeneous surface of CB-D, with a high porosity as well as the presence of the described “hydrogel effect”, would complicate the ordered arrangement of the stearic acid molecules on its surface. Oleic acid in turn, could be more intensively adsorbed (Fig. 8 b) than stearic acid because of possible interactions of the CB surface groups with the unsaturation via hydrogen bonding [29].

The adsorption activity ( $\text{mJ m}^{-2}$  of CB) for acetic acid with the four carbon blacks can be ranked as follows:

$$\text{CB-C} > \text{CB-A} > \text{CB-D} > \text{CB-B}, (25.2 \text{ mJ m}^{-2}) > (16.8 \text{ mJ m}^{-2}) > (6.8 \text{ mJ m}^{-2}) > (3.7 \text{ mJ m}^{-2}).$$

While the adsorption activities ( $\text{mJ m}^{-2}$  of CB) of valeric, hexanoic, stearic and oleic acid can be ranked as follows:

$$\text{CB-C} > \text{CB-A} \geq \text{CB-B} \geq \text{CB-D}$$

Valeric acid:  $(11.4 \text{ mJ m}^{-2}) > (2.1 \text{ mJ m}^{-2}) \geq (2 \text{ mJ m}^{-2}) \geq (1.8 \text{ mJ m}^{-2})$ ,

hexanoic acid:  $(10.1 \text{ mJ m}^{-2}) > (1.8 \text{ mJ m}^{-2}) = (1.9 \text{ mJ m}^{-2}) \leq (2.5 \text{ mJ m}^{-2})$ ,

decanoic acid:  $(8.4 \text{ mJ m}^{-2}) > (4 \text{ mJ m}^{-2}) = (1.9 \text{ mJ m}^{-2}) \leq (2.5 \text{ mJ m}^{-2})$ ,

oleic acid:  $(11.6 \text{ mJ m}^{-2}) > (4.2 \text{ mJ m}^{-2}) > (2.9 \text{ mJ m}^{-2}) \leq (3.1 \text{ mJ m}^{-2})$ .

The adsorption activities of stearic acid are ranked as follows:

$$\text{CB-A} > \text{CB-C} \geq \text{CB-B} > \text{CB-D}, (21.0 \text{ mJ m}^{-2}) > (16.4 \text{ mJ m}^{-2}) > (8.3 \text{ mJ m}^{-2}) > (1 \text{ mJ m}^{-2}).$$

In general, CB-C exhibits the greatest overall adsorption activity. This is because it has more active adsorption sites per unit surface area than

CB-A and CB-B, and is reflected in its surface elemental composition (Table 4). The relatively high volatile content (3.5%) of CB-C also reflects a high level of oxidised functional groups [13]. FTIR spectra revealed the presence of functional groups associated with carbonyl and carboxyl species (Fig. 1). The seemingly low intensity of this peak (shoulder of the C=C double bond stretching absorption) may understate its true significance in affecting adsorption activity. The high water content (2.56%), part of which may remain on the surface even after cleaning in the FMC overnight with dry heptane, is another factor affecting the adsorption behaviour of CB-C.

Although CB-D has the higher volatile content (8.5–12%), together with strong acidity, when dispersed in water (pH of  $3 \pm 1$ ), it shows the lowest adsorption activity with most of the fatty acids. FTIR and XPS analysis confirms the presence of acidic functional groups associated to carbonyl and carboxyl species (Fig. 1). The intensity of this peak is still low but nevertheless stronger than that of CB-C. The XPS analysis clearly indicates that

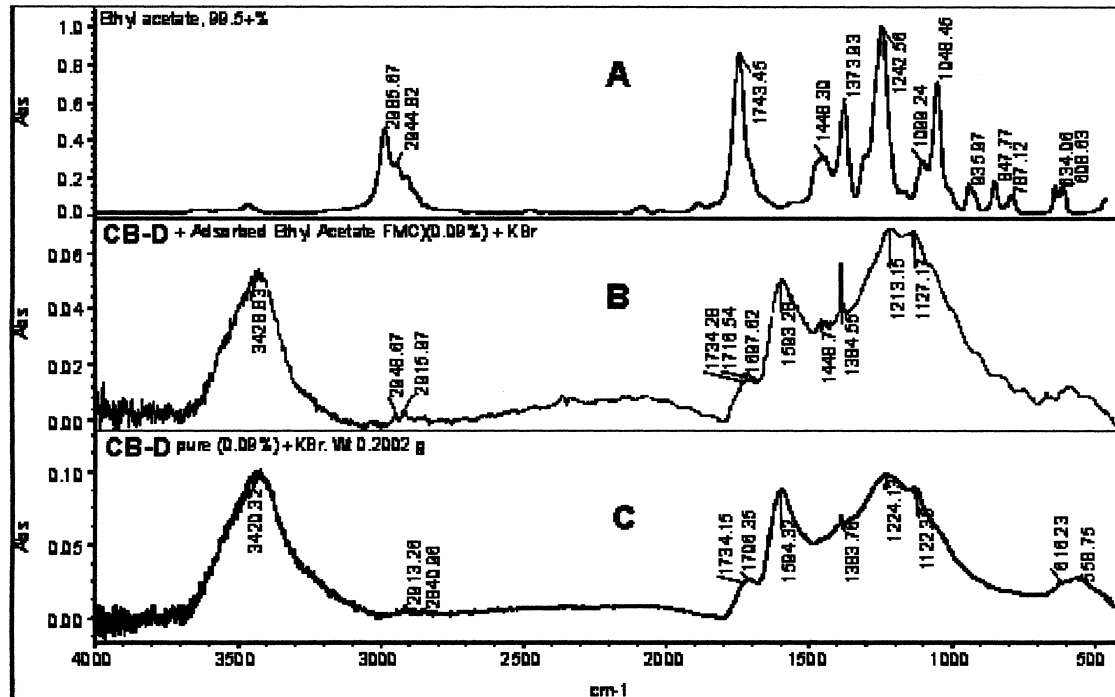


Fig. 17. Comparative FTIR spectra of: (A) pure ethyl acetate, (B) CB-D modified with ethyl acetate by FMC adsorption, (C) pure CB-D carbon black.

CB-D is the most highly oxidised sample. However, the surface area normalised FMC data is not consistent with this finding. This could be explained by the existence of a “hydrogel effect”. Such a “hydrogel effect” appears when there is a high concentration of polar groups on a surface; they interact with water molecules to form a gel-like structure (3D network by hydrogen bonding), which effectively blocks surface adsorption sites [30,31]. This reduction in adsorption activity, as measured by FMC, may also be related to the heptane wettability of the highly oxidised carbon black surface. If the surface is not properly wetted then only a limited area will be available for adsorption.

In addition, interactions between closely adjacent functional groups on the CB surface could result in the loss of adsorption activity; particularly when the interactions between these surface groups are stronger than the interactions between the surface groups and the adsorbate molecule. Thus, the functionalities, which are believed to be on the edges of the CB basal planes, would interact

with themselves, resulting in significantly reduced interactions with adsorbate molecules. In such a situation, it is possible that the surface activity of a CB will reach a maximum at a certain concentration of functional groups. Once this limit is exceeded, mutual interaction dominates and adsorption activity decreases. Of course, the activity would also depend on the nature of these functionalities. The porosity is also a factor to take into account, which would affect the adsorption of additives as described in the literature, especially with low molecular mass and phenolic compounds [28].

With CB-A and CB-B the adsorption energies of the fatty acids, phenol and benzoic acid shows a similar pattern. CB-A is more active than CB-B, despite the fact that the latter contains more oxygen functionalities (Table 4). A higher basic character can explain the higher activity of CB-A. This can be the reason for a higher irreversibility of the adsorption of fatty acids, when other factors such as porosity does not count because both CB's are non-porous. The same effect as for fatty acids was

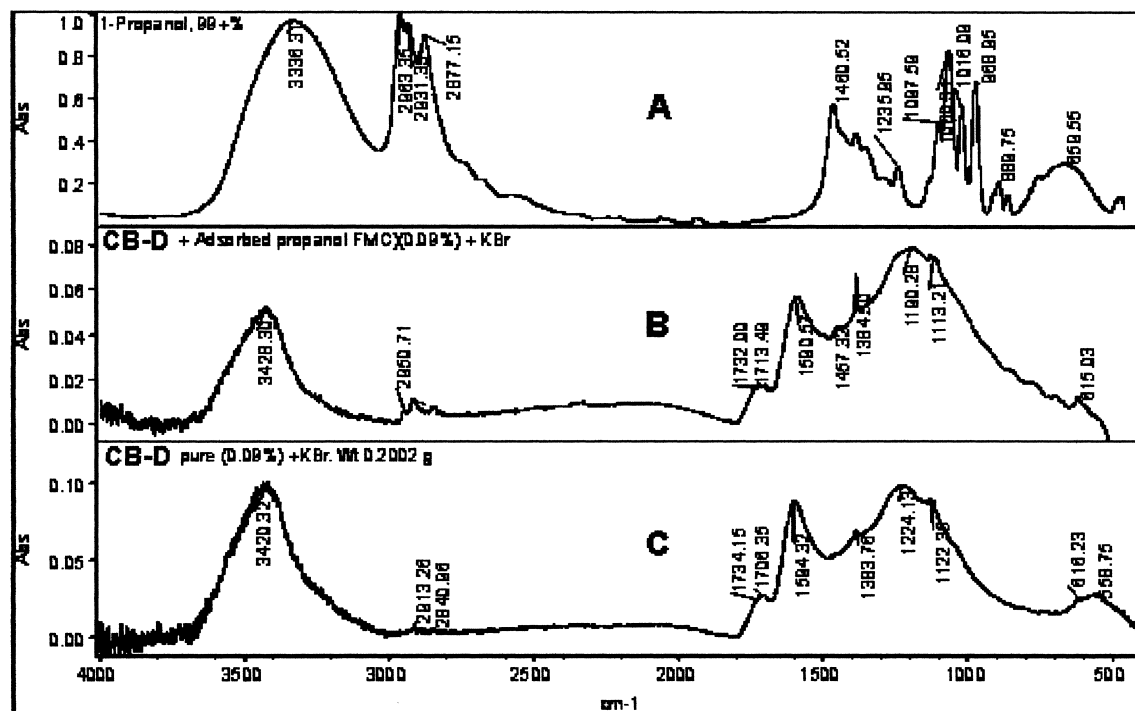


Fig. 18. Comparative FTIR spectra of: (A) pure 1-propanol, (B) CB-D modified with 1-propanol by FMC adsorption, (C) pure CB-D carbon black.

observed with phenol and benzoic acid, therefore indicating a strong contribution from acid–base interactions. With CB-B these adsorptions were shown to be reversible which implies that hydrogen bonding and dispersive interactions are mainly involved, rather than acid–base interactions.

### 3.2.3. FTIR spectra of carbon black treated in the FMC with carboxylic acids alcohols and ethyl acetate

In contrast to spectral data for the amine treated samples, the presence of adsorbed phenol was more easily detected on CB-D and CB-C. Absorptions at 752 and 690  $\text{cm}^{-1}$  can be obviously assigned to phenol adsorbed on CB-D (Fig. 14) whilst with CB-C some weak absorptions appear around 740 and 700  $\text{cm}^{-1}$ . Even CB-A and CB-B showed some evidence of adsorbed phenol, thus reflecting the strength of interaction with this probe (Fig. 15).

Only CB-D (0.9%) shows the presence of weakly adsorbed stearic acid with peaks at 2930  $\text{cm}^{-1}$  (C–H stretching vibration of  $\text{CH}_2$ ) (Fig. 16). The other probes such as propanol (Fig. 18) and ethyl acetate (Fig. 17) could also be resolved on the carbon black surfaces, although the absorptions are very weak.

## 4. Conclusions

FMC can be used to determine the interactions between the CB and the fatty acids. It is also evident that a difference in the chemical nature of the surface (chemical nature and concentration of CB surface functional groups) is related to the different behaviour observed in adsorption activity between the four carbon blacks. In general, increasing oxygen content results in a greater surface activity for polar additives. However, interactions between neighbouring surface groups can also decrease the surface activity of the carbon black by a so-called “hydrogel effect”. Furthermore, the surface structure and porosity of the black pigment is important and this can affect the dispersive component of the aromatic or fatty acid–CB surface interaction.

The high activity of aromatic compounds by comparison with fatty acids is as well probably due to the flat and planar aromatic structures of the former, as opposed to the alkyl chain fatty

acids. The more compact benzoic acid and phenol molecules may also easily fit into the CB pores (when porosity is present on the CB), thus allowing a greater surface area for adsorption. Phenol and benzoic acid showed greater retention that may reflect stronger dispersive interactions, because of the flat adsorption of these probes, as well as the strong contribution from acid–base interactions.

Increasing chain length from acetic acid to decanoic acid reduces the adsorption activity of fatty acids by an increasing solvation of the aliphatic chain. As well, a higher volume for the fatty acid molecule will nevertheless make the molecule less accessible to the CB porosity, when the acidity does not change substantially for relative fatty acids.

A further increase in the chain length reverses that effect because of the probable interaction between the aliphatic chains of the adsorbed molecules of stearic acid and the octadecanol resulting in an ordered distribution by crystallisation of the alkyl tails perpendicularly or flat wise to the carbon black surface. Such an interaction could be via Van der Waals forces between the aliphatic chains in addition of the hydrogen bonding of the acid group with the carbon.

In order to obtain a crystallisation of the alkyl tails, the linear structure and length of the aliphatic chain of the fatty acid molecule length (equal or superior to  $\text{C}_{17}$ ) are required, resulting in a higher energy of adsorption.

Although the presence of unsaturations reduce the ability of crystallisation of the fatty acid tails, and hence, the adsorption energy, they are bonding points to interact with the CB surface functionalities via hydrogen bonding or dispersive interactions.

X-ray Photoelectron spectroscopy analysis (XPS) has been shown to be a very powerful technique in order to obtain a more detailed characterisation of the carbon black surface functional groups.

FMC and FTIR shed some light on the manner in which the fatty acids can be adsorbed. Interaction by hydrogen bonding and or acid base between carboxyl and hydroxyl containing groups on the carbon black surface with the carboxylic groups of the fatty acids is one mode of adsorption. Dispersive interactions between the aliphatic

chain tails and the surface basal graphene layers of the CB, has also been shown to occur.

Other functional groups containing labile H (hydroxyl and phenolic) of the CB can also interact via H bonding with the aromatic structures of the fatty acids.

Other kinds of acid/base polar interactions can be present, such as proton transfer complex and ion pair formation, depending on the relative acidic–basic strength of the absorbent and adsorbate [29].

The reversibility of the adsorption is also related to the relative acidic or basic character of the adsorbate and adsorbent (CB).

## References

- [1] Peña JM, Allen NS, Edge M, Liaw CM. Factors affecting the adsorption of stabilisers on to carbon black (flow micro-calorimetry studies). *Journal of Vinyl and Additive Technology* 2000; 6(2).
- [2] Peña JM, Allen NS, Edge M, Liaw CM, Valange B. Factors affecting the adsorption of stabilisers on to carbon black (flow micro-calorimetry studies). *International Symposium Eurofillers*, September 1999.
- [3] Peña JM, Allen NS, Liaw CM, Edge M, Noiset O, Valange B, Santamaria F. Factors affecting the adsorption of stabilisers on to carbon black (flow micro-calorimetry studies), 1. Primary phenolic antioxidants. *J Mat Sci*, in press.
- [4] Peña JM, Allen NS, Liaw CM, Edge M, Noiset O, Valange B, Santamaria F. Factors affecting the adsorption of stabilisers on to carbon black (flow micro-calorimetry studies), 2. HALS. *J. Mat. Sci.*, in press.
- [5] Peña JM, Allen NS, Liaw CM, Edge M, Noiset O, Valange B. Factors affecting the adsorption of stabilisers on to carbon black (flow micro-calorimetry studies), 3. Surface activity study using acid/base model probes. *J Mat Sci*, in press.
- [6] Peña JM, Allen NS, Liaw CM, Edge M, Valange B. Factors affecting the adsorption of stabilisers on to carbon black (flow micro-calorimetry studies), 4. Secondary antioxidants. *Polym Degrad Stab*, in press.
- [7] Peña JM, Allen NS, Edge M, Liaw CM, Valange B. Studies of synergism between carbon black and stabilisers in LDPE oxidation: thermal degradation by design of experiments (DOE). *Polym. Degrad. Stab.*, in press.
- [8] Peña JM, Allen NS, Edge M, Liaw CM, Valange B. Studies of synergism between carbon black and stabilisers in LDPE Photodegradation by Design of Experiment (DOE). *Polym Degrad Stab*, in press.
- [9] Bandyopadhyay S, DE PP, Tripaty DK. Effect of chemical interaction between surface oxidized carbon black and carboxylated nitrile rubber on dynamic properties). *Journal of Applied Science* 1995;58:719–27.
- [10] Wolfschewenger J, Hauer A, Gahleitner MG, Neibl W. *Proceedings Eurofillers 97*. Manchester: British Plastics Federation, 1997. p. 375–77.
- [11] Liaw CM, Childs A, Allen NS, Edge M, Franklin KR, Collopy DG. *Polym Degrad Stab* 1999;65:207.
- [12] D'Silva AP. Adsorption of antioxidants by carbon blacks. *Carbon* 1998;36(9):1317–25.
- [13] Donnet J-B, Bansal RC, Wang M. *Carbon black, science and technology*. New York: Marcel Dekker, 1993.
- [14] Dannenberg EM. *Carbon black*, Cabot research paper, *Encyclopaedia of chemical technology*, vol. 4. New York: Wiley, 1992.
- [15] Fabish TJ, Schleifer DE. Surface chemistry and the carbon black work function. *Carbon* 1984;22(1):19–38.
- [16] Polley MH, Schaeffer WD, Smith WR. *J Am Chem Soc* 1951;73:2161.
- [17] Wang M-J, Wolff S, Donnet J-B. *Rubber Chem Technol* 1991;64:714.
- [18] Avrom I. *Carbon Black*. Medalia, NY: Medalia Associates, 1991.
- [19] Fowkes FM. In: Mittal KL, Anderson Jr. HR, editors. *Acid–base interactions*. VPS, 1991. p. 93–115.
- [20] Ashton DP, Briggs D. Particulate filled polymer composites. In: Rothon RN, editor. *Analytical technique for characterising filler surfaces*. Longman Scientific and General, Harlow, 1995. p. 90–105.
- [21] Liaw CM, Rothon RN, Hurst SJ, Lees GC. *Composite Interfaces* 1998;5:503–14.
- [22] Cabot North American Technical Report S-136, Cabot-Corp, 1999.
- [23] Boehm HP. Some aspects of the surface chemistry of carbon black and others carbons. *Carbon* 1994;32(5):759–69.
- [24] Sutherland I, Sheng E, Bradley RH. Effects of ozone oxidation on carbon black surfaces. *Journal of Materials Science* 1996;31:5651–5.
- [25] O'Reilly JM, Mosher RA. Functional groups in carbon black by FTIR spectroscopy. *Carbon* 1983;21(1):47–51.
- [26] Papirer E, Lacroix R. *Carbon* 1994;32:1341–58.
- [27] Vollhardt C, editor. *Organic chemistry*. New York: Omega, 1990.
- [28] Asakawa T, Ogino K, Yamabe K. Adsorption of phenol on surface-modified carbon black from its solutions. II Influence of surface chemical structure of carbon on adsorption of phenol. *Bull Chem Soc Jpn* 1985;58:2009–14.
- [29] Vinogradov SN, Linnell RH. *Hydrogen bonding*. New York: Van Nostrand Reinhold Company, 1971.
- [30] Wesslén B, Kober M. *Biomaterials* 1994;15(4):278–84.
- [31] Österberg E, Bergström K. *Applied Surface Science* 1995;64:197–203.
- [32] *Handbook of chemistry and physics*. CRC Press, New York. p. D-117, E-51.